

NONLINEAR OPTICAL PHENOMENA https://doi.org/10.1070/QEL16856

Enhancement of the sensitivity of the light-induced drift effect to interatomic interaction potentials using a mixture of two buffer gases

A.I. Parkhomenko, A.M. Shalagin

Abstract. **Based on five different nonempirical (calculated *ab initio*) interaction potentials for pairs of colliding Li–Ne particles and three different interaction potentials for pairs of colliding Li–Ar particles, we have theoretically investigated the spectral features of the light-induced drift (LID) rate of Li atoms in the buffer Ne gas in a mixture of buffer Ne + Ar gases. The calculations of LID of Li atoms in the buffer Ne gas for two interaction potentials predict anomalous LID and, as a result, strong sensitivity of the spectral shape of the LID lines to the differences in these potentials. For three other potentials (out of the five in question), the shape of the LID line of Li atoms in Ne is insensitive to the shape of the potential, since calculations with these potentials predict a normal LID effect. In this case, as it turned out, by adding a small fraction (approximately 10 %) of Ar to Ne, one can go from normal LID to anomalous LID and thereby radically increase the sensitivity of the LID line shape of Li atoms to the difference in these interaction potentials. The results obtained enable high-precision testing of the interatomic interaction potentials in experiments on anomalous LID.**

Keywords: *light-induced drift, optical excitation, collisions, buffer gas, interatomic interaction potential.*

1. Introduction

The effect of a light-induced drift (LID) is the occurrence of directional movement (drift) of particles that absorb light radiation and are in a mixture with a buffer gas [1, 2]. This drift arises due to two circumstances: selectively in terms of the rate of excitation of particles by light (due to the Doppler effect) and the difference in the times of translational relaxation of resonant particles in the ground and excited states when they collide with buffer particles. The drift motion of resonant particles can be carried out both in the direction of radiation propagation and in the opposite direction. To date, the LID effect has been experimentally registered for almost two dozen different objects – atoms and molecules (see, for example, [3–9] and references therein). Theoretically, with laser excitation, the drift velocity due to the LID effect can reach thermal velocity [10]. It was experimentally shown that atoms under the action of LID can drift at a velocity of 50 m s^{-1} [11].

An important characteristic of the LID effect is the dependence of the drift velocity on the radiation frequency (the shape of the LID line). According to the line of the LID line observed in experiments, the effect has been classified as 'normal' and 'anomalous' LID.

The normal effect is well described by the LID theory with velocity-independent transport collision frequencies of resonant particles in the ground and excited states with buffer particles. Under the normal effect, the LID line shape has the simplest form and is completely determined by the absorption spectrum of the drifting particles. In particular, under excitation by radiation from particles on an isolated transition (two-level particles), the normal LID line has a characteristic dispersion-like (tilde-like) shape [3–7].

Anomalous LID has a much more complex line shape. Many experimental [8, 9, 12–18] and theoretical [8, 15, 17, 19–29] papers have been devoted to the study of anomalous LID. It was found that anomalies are observed in cases where the transport collision frequencies of resonant particles with buffer particles at the combining (affected by radiation) levels are close to each other. It turned out that under these conditions, the occurrence of anomalous LID is due to the dependence of the transport characteristics of the absorbing particle on its velocity. Because the collision transport frequencies are determined by the interaction potentials of resonant and buffer particles, the line shape of anomalous LID is extremely sensitive to small changes in the interaction potentials. This allows in LID experiments the precision testing of interatomic interaction potentials used to calculate the spectral waveform of anomalous LID, and, therefore, the possibility of relatively simple experimental testing of the accuracy of various theoretical models of interaction potentials.

Based on several known non-empirical (calculated ab initio) interatomic interaction potentials for pairs of colliding Li–Ne particles, we theoretically predicted and calculated anomalous LID of lithium atoms in the neon buffer [29]. The results of this work showed that, in the region of anomalous LID, even a small difference in the interatomic interaction potentials of resonant and buffer particles is strongly manifested in the frequency dependence of the drift velocity. In the regions of normal LID, the shape of its line is insensitive to the difference in interaction potentials.

In this paper, we report a theoretical study of the spectral features of the LID velocity of Li atoms in an inert buffer Ne gas and in a binary buffer mixture of inert Ne + Ar gases. The LID calculations are based on five different non-empirical interaction potentials for pairs of colliding Li–Ne particles

A.I. Parkhomenko Institute of Automation and Electrometry, Siberian Branch, Russian Academy of Sciences, prosp. Akad. Koptyuga 1, 630090 Novosibirsk, Russia; e-mail: par@iae.nsk.su;
A.M. Shalagin Institute of Automation and Electrometry, Siberian Branch, Russian Academy of Sciences, prosp. Akad. Koptyuga 1, 630090 Novosibirsk, Russia; Novosibirsk State University, ul. Pirogova 2, 630090 Novosibirsk, Russia; e-mail: shalagin@iae.nsk.su

Received 11 October 2018; revision received 20 November 2018
Kvantovaya Elektronika **49** (7) 683–688 (2019)
Translated by I.A. Ulitkin

[30–34] and three different non-empirical interaction potentials for pairs of colliding Li–Ar particles [30, 33, 35]. The calculations of LID of Li atoms in the buffer Ne gas have shown that for some interaction potentials, the shape of the LID line will be insensitive to their difference, since they predict LID to be close to normal. In this case, as it turned out, it is possible to switch to the region of anomalous LID and thereby significantly increase the sensitivity of the LID line shape to the difference of these interaction potentials by adding a small fraction of Ar gas to the initial buffer medium of Ne gas.

2. Drift velocity

Lithium has two stable isotopes: ^{7}Li (abundance of 92.5%) and ^{6}Li (abundance of 7.5%) [36]. The isotopic frequency shift of the spectral lines of the main ^{7}Li isotope relative to the frequencies of the lines of the ^{6}Li isotope is such that when the laser radiation frequency is tuned to the D_2 line of ^{7}Li, only one main ^{7}Li isotope interacts with radiation. Bearing in mind this situation, we will further consider LID of ^{7}Li atoms in the case of excitation of the D_2 transition of ^{7}Li atoms.

To calculate the LID velocity of ^{7}Li atoms, it is quite possible to use a three-level model of absorbing particles (Fig. 1). Here the levels n, k are the components of the hyperfine structure of the $2^2S_{1/2}$ ground state. Level m corresponds to the excited $2^2P_{3/2}$ electronic state. For ^{7}Li atoms, the hyperfine splitting of the ground state, $\omega_{kn} = 5.049 \times 10^9$ s^{-1} [36], is comparable to the Doppler width of the resonance line, and therefore the ground state is modelled by two levels, n and k. Level m models a group of levels that are components of the hyperfine structure of the excited $2^2P_{3/2}$ state. Such a simulation of a group of levels by a single level is possible because for ^{7}Li atoms the hyperfine splitting in this excited state is small compared with the Doppler width of the resonance line.

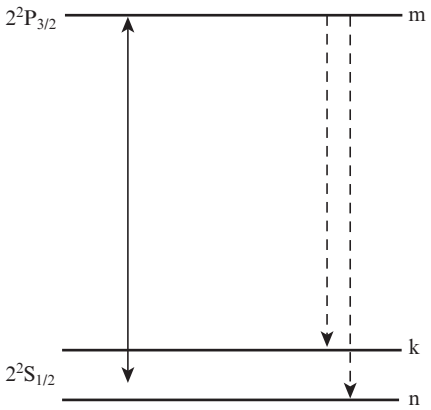

Figure 1. Energy level diagram. The solid arrow indicates the transition under the action of radiation, and the dashed arrows show spontaneous radiative transitions.

For the LID velocity of ^{7}Li atoms (simulated by a three-level scheme, Fig. 1) in the inert atmosphere of buffer gases, we obtained the expression [29]:

$$\boldsymbol{u}_L = \frac{\boldsymbol{k}}{k}\frac{2BI}{\sqrt{\pi}k^2v_T^3}\left[\Omega_n\frac{N_n}{N}\int_{|\Omega_n|/k}^{\infty}\tau(v)v\exp\left(-\frac{v^2}{v_T^2}\right)dv + \right.$$
$$\left. + \left[\Omega_k\frac{N_k}{N}\int_{|\Omega_k|/k}^{\infty}\tau(v)v\exp\left(-\frac{v^2}{v_T^2}\right)dv\right], \quad (1)$$

where

$$\tau(v) = \frac{\nu_n(v) - \nu_m(v)}{\nu_n(v)[\Gamma_m + \nu_m(v)]};\ \frac{N_n}{N} = \left[1 + \frac{5}{3}\exp\left(\frac{\Omega_k^2 - \Omega_n^2}{k^2v_T^2}\right)\right]^{-1};$$
$$\frac{N_k}{N} = 1 - \frac{N_n}{N};\ \ B = \frac{\lambda^2\Gamma_m}{2\hbar\omega};\ \ \Omega_i = \omega - \omega_{mi};\ \ i = n,k; \quad (2)$$

$\nu_n(v)$ and $\nu_m(v)$ are the transport frequencies of collisions of resonant particles in the ground and excited states with buffer particles; v is the velocity of resonant particles; B is the second Einstein coefficient for absorption [37]; N_n/N and N_k/N are the relative populations of the sublevels n and k of the hyperfine structure of the ground state; ω, λ, $\boldsymbol{k}$, and I are the frequency, wavelength, wave vector, and intensity of monochromatic radiation; ω_{mi} is the transition frequency m → i; Γ_m is the spontaneous decay rate of the excited level m; $v_T = (2k_BT/M)^{1/2}$ is the most probable velocity of absorbing particles; M is the mass of particles absorbing radiation; k_B is the Boltzmann constant; and T is the temperature.

Expression (1) for the drift velocity is valid in the case of large Doppler broadening.

$$\Gamma \ll kv_T \quad (3)$$

and under conditions of low intensity radiation

$$\varkappa \equiv \frac{BI}{\pi\Gamma(\Gamma_m + \nu_m)} \ll 1, \quad (4)$$

where $\Gamma = \Gamma_m/2 + \gamma$ is the homogeneous half width of the absorption line, which is the sum of the spontaneous ($\Gamma_m/2$) and collisional (γ) half widths. Case (3) is most interesting for the problem in question, since anomalous LID maximally manifests itself at a large Doppler broadening. Under conditions (4) of weak radiation intensity, the distribution of populations with respect to velocities on the hyperfine components n, k in the ground state is close to Maxwellian. The value of $\varkappa$ has the meaning of the saturation parameter: It characterises the degree of population levelling in particles with resonant velocities ($\Omega_i = \boldsymbol{kv}$).

The relation of the collision transport frequency $\nu_i(v)$ (i = m, n) in (2) with the characteristics of the elementary scattering event is given by the well-known formula [38]

$$\nu_i(v) = \frac{\mu}{M}\frac{N_b\bar{v}_b}{\sqrt{\pi}v^3}\int_0^{\infty}u^2\exp\left(-\frac{u^2+v^2}{\bar{v}_b^2}\right)F(uv)\sigma_i(u)du, \quad (5)$$

where

$$F(uv) = \frac{2uv}{\bar{v}_b^2}\cosh\frac{2uv}{\bar{v}_b^2} - \sinh\frac{2uv}{\bar{v}_b^2};$$
$$\mu = \frac{MM_b}{M+M_b};\ \ \bar{v}_b = \sqrt{\frac{2k_BT}{M_b}}; \quad (6)$$

N_b and M_b are the concentration and mass of buffer particles; u is the relative velocity of the resonant and buffer particles before the collision; and $\sigma_i(u)$ is the scattering transport cross section of an absorbing particle in state i on a buffer particle.

The cross sections $\sigma_i(u)$ are calculated using the interaction potentials of the absorbing and buffer particles.

As noted in the Introduction, anomalous LID can arise when the transport collision frequencies $\nu_m(v)$ and $\nu_n(v)$ of resonant particles in excited and ground states with buffer particles are close to each other. The reason for the appearance of anomalous LID is the difference in the dependences of $\nu_m(v)$ and $\nu_n(v)$ and, as a result, the possibility of changing the sign of the difference in the collision transport frequencies $\Delta\nu(v) \equiv \nu_m(v) - \nu_n(v)$. In this case, absorbing particles with both positive and negative $\Delta\nu(v)$ values contribute to the drift velocity $\boldsymbol{u}_L$. This can lead to a strong difference in the shape of the LID line from that predicted by the theory of the normal LID effect, which does not take into account the dependence of the transport collision frequencies on the velocity.

If the frequencies $\nu_m(v)$ and $\nu_n(v)$ are very different from each other, then the drift velocity $\boldsymbol{u}_L$ as a function of the emission frequency corresponds to normal LID and is well described by its theory with velocity-independent transport collision frequencies, i.e. when frequencies $\nu_i(v)$ (i = m, n) in expression (1) are replaced by the average transport frequency

$$\nu_i^{tr} = \frac{2}{v_T^2}\int (\boldsymbol{nv})^2 W(\boldsymbol{v})\nu_i(v)\,d\boldsymbol{v}$$

$$= \frac{8}{3\sqrt{\pi}}\frac{\mu}{M}\frac{N_b}{u_T^5}\int_0^\infty u^5 \exp\left(-\frac{u^2}{u_T^2}\right)\sigma_i(u)\,du, \qquad (7)$$

where $u_T = (2k_BT/\mu)^{1/2}$ is the most probable velocity of the relative motion of the absorbing and buffer particles; and n is the unit vector in an arbitrarily chosen direction. The average transport frequency ν_i^{tr} is related to the diffusion coefficient D_i of particles in the state i by a simple formula [3, 38]:

$$D_i = \frac{v_T^2}{2\nu_i^{tr}}. \qquad (8)$$

In calculating the LID velocity of the atoms in a mixture of two different buffer gases, for $\tau(v)$ in formula (2) we assume

$$\nu_i(v) = \nu_{1i}(v) + \nu_{2i}(v), \quad i = m, n, \qquad (9)$$

where subscripts 1 and 2 denote the sort of buffer particles. Similarly, the total shock half-width of the absorption line γ is equal to the sum of the half-widths γ_1 and γ_2, caused by the shock effect of the buffer particles of sorts 1 and 2.

3. Abnormal LID of lithium atoms

Using formulas (1), (2) and (5), we numerically investigated LID of ^{7}Li atoms in inert buffer Ne and Ar gases. According to the NIST database [39], for lithium atoms, the spontaneous decay rate Γ_m of the excited $2^2P_{3/2}$ state is 3.69×10^7 s^{-1}, and the wavelength of the D_2 line is λ = 670.8 nm. The homogeneous half width of the absorption line, $\Gamma = \Gamma_m/2 + \gamma$, was determined according to [40] for the collision broadening coefficients β_{Ne} = 5.50 MHz Torr^{-1} for Li atoms in the Ne atmosphere and β_{Ar} = 8.61 MHz Torr^{-1} for Li atoms in the Ar atmosphere. The collision transport frequencies $\nu_m(v)$ and $\nu_n(v)$ for Li atoms in excited and ground states with Ne and Ar atoms were calculated numerically by formula (5) using five different non-empirical (calculated ab initio) interaction potentials for pairs of colliding Li–Ne particles [30–34] and three different non-empirical interaction potentials for pairs of colliding Li–Ar particles [30, 33, 35]. Tabularly specified interaction potentials were interpolated by cubic splines.

Figure 2 presents the dependences [calculated by formula (5)] of the relative difference of the transport collision frequencies $[\nu_m(v) - \nu_n(v)]/\nu_n(v)$ on the velocity v for the Li atoms in the excited and ground states with Ne atoms (Fig. 2a) and Ar atoms (Fig. 2b) at T = 600 K. Formula (1) shows that, due to the factor $v\exp(-v^2/v_T^2)$, the main contribution to the integral for the drift velocity $\boldsymbol{u}_L$ is made by particles with velocities $v \sim v_T$. For pairs of colliding Li–Ne particles for two potentials [32, 33], the sign of the difference between the collision frequencies $\nu_m(v) - \nu_n(v)$ changes in the region $v \sim v_T$ [curves (*4*) and (*5*) in Fig. 2a]; therefore, in the vicinity T = 600 K, calculations using these potentials will predict anomalous LID of Li atoms in the Ne buffer medium. For three potentials [30, 31, 34], the sign of the difference in collision frequencies $\nu_m(v) - \nu_n(v)$ changes in the range $v \sim 2v_T$ [curves (*1*), (*2*) and (*3*) in Fig. 2a]; therefore, at a temperature T = 600 K, calculations for these potentials will predict weakly anomalous (close to normal) LID of Li atoms. For pairs of colliding Li–Ar particles, all three interaction potentials [30, 33, 35] do not change the sign of the difference in collision frequencies (Fig. 2b); therefore, at T = 600 K, normal LID of

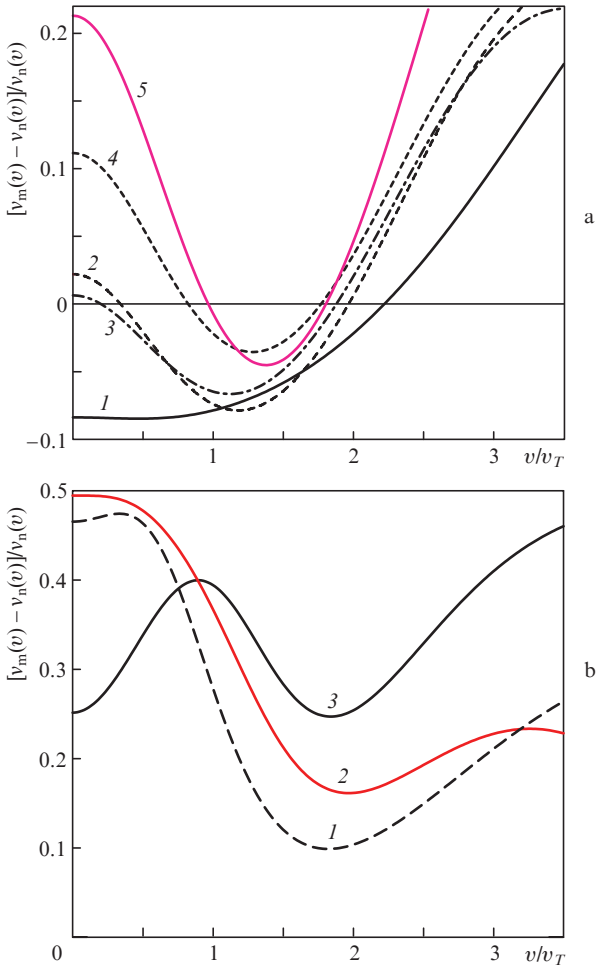

Figure 2. Velocity as a function of the relative difference of the transport collision frequencies $[\nu_m(v) - \nu_n(v)]/\nu_n(v)$ of Li atoms in the excited and ground states with (a) Ne and (b) Ar atoms; T = 600 K. Calculations of potentials are presented (a) from (*1*) [30], (*2*) [31], (*3*) [34], (*4*) [32] and (*5*) [33] and also (b) from (*1*) [30], (*2*) [35] and (*3*) [33] (b).

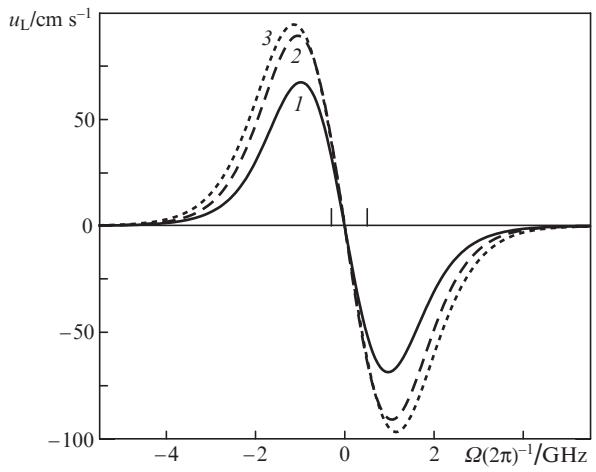

Figure 3. LID velocity projections on the radiation direction $u_L \equiv \boldsymbol{k}\boldsymbol{u}_L/k$ as functions of the detuning of the radiation frequency Ω for ^{7}Li atoms in the Ar buffer gas in the case of excitation of the D_2 transition of ^{7}Li atoms at $T = 600$ K, $I = 40$ mW cm^{-2} and $p_{buf} = 5$ Torr. Calculations of potentials are taken from (*1*) [30], (*2*) [35] and (*3*) [33]. Vertical segments denote frequencies resonant to the m–n and m–k transitions.

Li atoms in an Ar buffer medium is realized for these potentials.

Figures 3 and 4 present the results of numerical calculations [using formula (1)] of the projection of the LID velocity on the radiation direction $u_L \equiv \boldsymbol{k}\boldsymbol{u}_L/k$ as a function of the frequency detuning Ω for ^{7}Li atoms in the buffer Ar gas (Fig. 3), in the buffer Ne gas (Fig. 4a) and in the mixture of buffer Ne + Ar gases (Figs 4b–4d) with a fraction of neon in the mixture, $\xi_{Ne} = 0.89$ [$\xi_{Ne} = N_{Ne}/(N_{Ne} + N_{Ar})$, where N_{Ne} and N_{Ar} are the concentrations of neon and argon]. All calculations were performed for the case of the excitation of the D_2 transition of ^{7}Li atoms at the monochromatic radiation intensity $I = 40$ mW cm^{-2}, the buffer gas pressure $p_{buf} = 5$ Torr and the temperature $T = 600$ K [with these parameters, conditions (3) and (4) of applicability of formulas (1) are well fulfilled: $\Gamma/(kv_T) = 0.02$ and $\varkappa = 0.2$]. For the radiation frequency detuning Ω, we have

$$\Omega = \omega - \omega_0, \quad \omega_0 = \frac{3\omega_{mn} + 5\omega_{mk}}{8}. \tag{10}$$

The frequency ω_0 corresponds to the 'centre of gravity' of the transition frequencies ω_{mn} and ω_{mk}, taking into account the

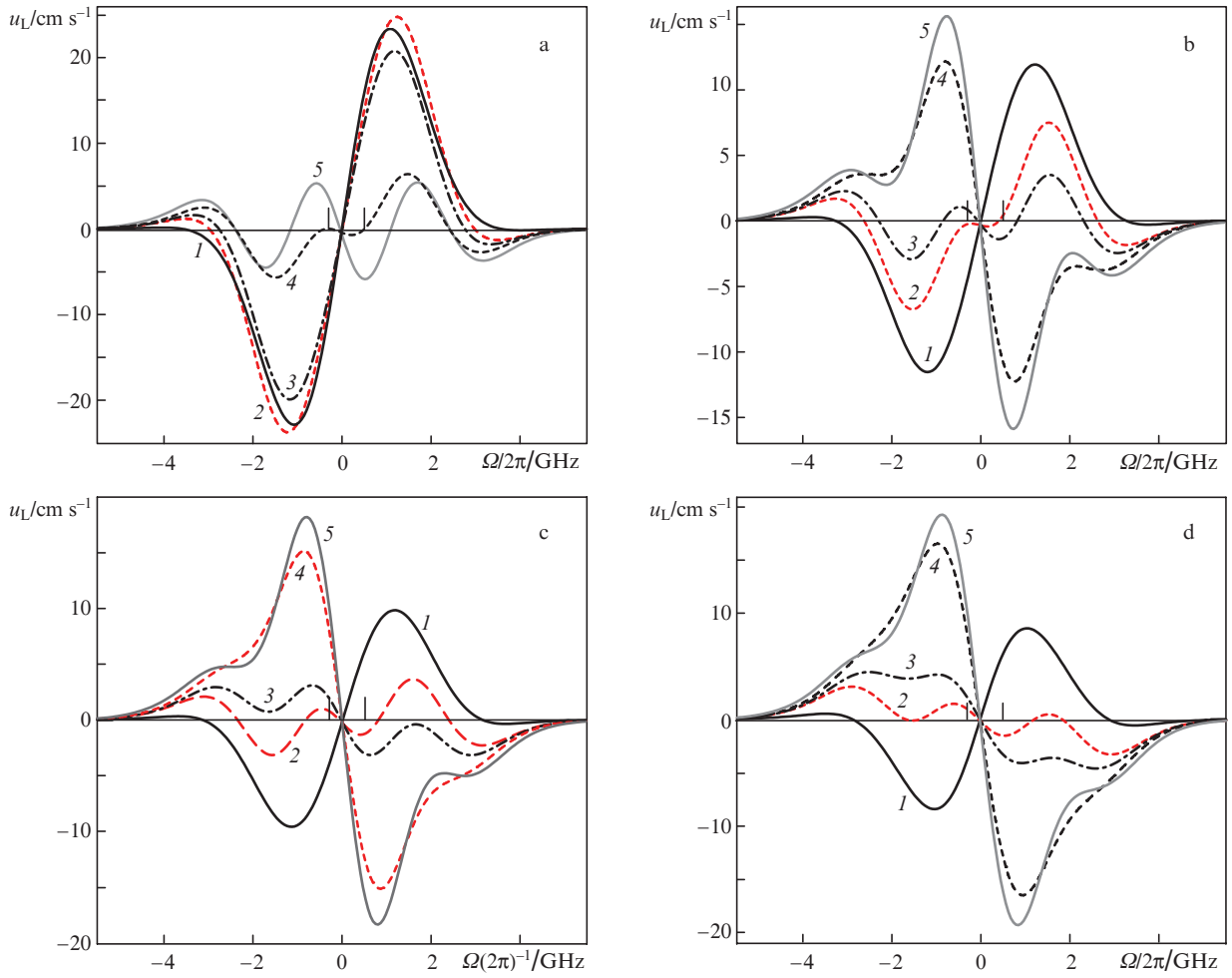

Figure 4. LID velocity projections on the radiation direction $u_L \equiv \boldsymbol{k}\boldsymbol{u}_L/_k$ as functions of the detuning of the radiation frequency Ω for ^{7}Li atoms (a) in the Ne buffer gas and (b–d) in the mixture of Ne + Ar buffer gases with a fraction of neon $\xi_{Ne} = 0.89$ in the case of excitation of the D_2 transition of ^{7}Li atoms at $T = 600$ K, $I = 40$ mW cm^{-2} and $p_{buf} = 5$ Torr. For a system of colliding Li–Ne particles, the calculation of potentials are taken from (*1*) [30], (*2*) [31], (*3*) [34], (*4*) [32] and (*5*) [33]. For a system of colliding Li–Ar particles, the calculation of potentials are taken from (b) [30], (c) [35] and (d) [33]. Vertical segments denote frequencies resonant to the m–n and m–k transitions.

statistical weights of the levels n and k. In the region of normal LID [when a substitution $\nu^{tr}_{n,m}(v) \to \nu^{tr}_{n,m}$) can be made in (1)], the drift velocity $\boldsymbol{u}_L$ vanishes only at point $\Omega = 0$ [41].

One can see from Fig. 3 that calculations using each of the three interaction potentials [30, 33, 35] predict the occurrence of normal LID of ^{7}Li atoms in the Ar atmosphere. The LID line shape is insensitive to the difference in interaction potentials: For each potential, the LID line has the same characteristic dispersion-like (tilde-shaped) shape, and the drift velocity $\boldsymbol{u}_L$ vanishes only at point $\Omega = 0$. The dependence of the results of the LED velocity calculations on the interaction potentials is rather weak and manifests itself only in a small change in the maximum drift velocity.

A completely different situation with the sensitivity of the LID line shape to the difference in interaction potentials arises in the case of LID of ^{7}Li atoms in the buffer Ne gas (Fig. 4a) and in the mixture of Ne + Ar buffer gases (Figs 4b–4d). The LID velocity calculations shown in Fig. 4 were performed on the basis of five different interaction potentials for pairs of colliding Li–Ne particles [30–34] and three different interaction potentials for pairs of colliding Li–Ar particles [30, 33, 35].

In the case of LID of ^{7}Li atoms in the Ne atmosphere, calculations for two potentials [32, 33] predict anomalous LID [curves (*4*) and (*5*) in Fig. 4a], and calculations for three potentials [30, 31, 34] predict slightly anomalous (close to normal) LID [curves (*1*), (*2*) and (*3*) in Fig. 4a]. For ^{7}Li atoms, the drift velocity as a function of the radiation frequency may have, depending on the potentials used for the calculations, one, three, or even five [curve (*5*) in Fig. 4a] zeros. Very important is the fact that the shape of the LID line [the dependence of $u_L(\Omega)$] is extremely sensitive to the difference in some interaction potentials used to calculate the LID velocity. If in the experiment on LID of lithium atoms in neon, the shape of the LID line is close to the shape of curve (*4*) or (*5*), then this clearly demonstrates in favour of the interaction potentials corresponding to these curves [32] or [33]. Curves (*1*), (*2*) and (*3*) corresponding to the interaction potentials from [30, 31, 34], respectively, are close to each other; therefore, the unequivocal choice between these potentials is difficult.

It turns out that the sensitivity of the shapes of curves (*1*), (*2*) and (*3*) to the difference in interaction potentials from [30, 31, 34] can be greatly increased by moving to the anomalous LID region by adding a small fraction of Ar gas to the original buffer Ne gas. Figures 4b–4d presents the results of calculations of the LID velocity of ^{7}Li atoms in a mixture of Ne + Ar buffer gases with a fraction of neon in a mixture $\xi_{Ne} = 0.89$. It can be seen that in the mixture of Ne + Ar buffer gases, the shapes of curves (*1*), (*2*) and (*3*) turn out to be very sensitive to the difference in interaction potentials from [30, 31, 34] for pairs of colliding Li–Ne particles. At the same time, the sensitivity of the shapes of these curves to the difference in interaction potentials from [30, 33, 35] for pairs of colliding Li–Ar particles increases (cf. Fig. 3 with Figs 4b–4d). A preliminary conclusion about the accuracy of the interaction potentials can be made by comparing the values of $(D_m - D_n)/D_n$ of relative diffusion coefficients of lithium atoms in the excited and ground states calculated in the present work and measured in experiments [42] by light-induced diffusive pulling (pushing) (LDP) in the atmospheres of inert buffer gases of neon and argon. In the LDP effect [43], unlike the LID effect, spectral anomalies do not occur [44]. The magnitude of the LDP effect is always proportional to the relative difference of the average collision transport frequencies $(\nu^{tr}_m - \nu^{tr}_n)/\nu^{tr}_n$ [and hence the relative difference of the diffusion coefficients $(D_m - D_n)/D_n$ in the excited and ground states of resonant atoms with buffer particles]. For Li atoms in the Ne atmosphere at temperature $T = 600$ K, the value measured in experiment [42] $(D_m - D_n)/D_n = 0.026 \pm 0.006$. The calculated values of $(D_m - D_n)/D_n$ for potentials from [34, 30, 33, 32, 31] are equal, respectively, to 0.026, 0.051, –0.009, –0.0014 and 0.064. For Li atoms in the Ar atmosphere at temperature $T = 600$ K, the value of $(D_m - D_n)/D_n$ measured in experiment [42] is equal to -0.23 ± 0.02. The calculated values of $(D_m - D_n)/D_n$ for the potentials from [33, 30, 35] are equal to –0.237, –0.144 and –0.199, respectively. Thus, the interaction potential from [34] for pairs of colliding Li–Ne particles and the interaction potential from [33] for pairs of colliding Li–Ar particles perfectly describe the experimental results [42], and the LID calculation of Li atoms based on them should be given priority [curves (*3*) in Fig. 3 and Figs 4a and 4d).

An important characteristic of the potential testing method by the LID line shape is its sensitivity to the difference in the interaction potentials used. Figure 5 shows the interaction potentials from [31, 34] for pairs of colliding Li–Ne particles, according to which curves (LID line shapes) (*2*) and (*3*) in Figs 4b–4d were calculated. Visually, the potentials in Fig. 5 from [31, 34] differ slightly. Nevertheless, a comparison of Fig. 5 and curves (*2*) and (*3*) in Figs 4b–4d shows that even a small difference in the interatomic interaction potentials of resonant and buffer particles is strongly manifested in the frequency dependence of the drift velocity in the anomalous LID region.

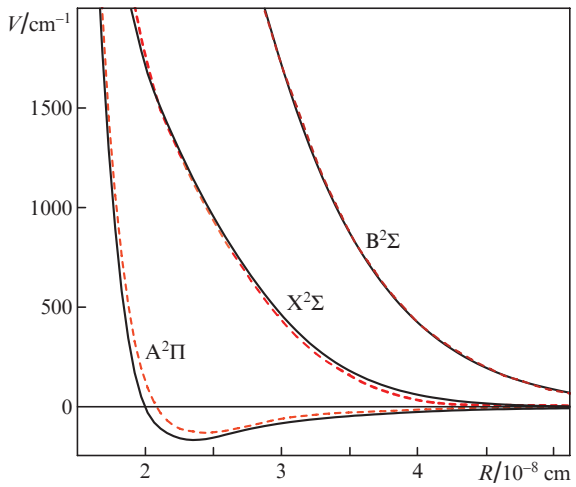

Figure 5. Interaction potentials for a system of colliding Li–Ne particles. The interaction of unexcited Li atoms (^{2}S state) with Ne atoms (^{1}S ground state) corresponds to the molecular term $X^2\Sigma$, and the excited Li atoms (^{2}P state) corresponds to the terms $A^2\Pi$ and $B^2\Sigma$. The solid curves are the potentials from [31], and the dashed curves are the potentials from [34].

It should be noted that in the dependence of the LID velocity on the radiation frequency, it is not the interaction potentials that manifest themselves, but the difference in the interaction potentials of excited and unexcited resonant particles with buffer particles. At present, other methods for testing the interaction potential difference are unknown to us.

In this paper, we showed the possibility of artificially creating conditions for the manifestation of anomalous LID by using a mixture of two buffer gases. This dramatically increases the sensitivity of the testing of the interaction potentials. It is difficult to say to what degree this method is universal, since the data on the interaction potentials of excited atoms with different buffer particles are still scarce.

4. Conclusions

Based on five different interaction potentials for pairs of colliding Li–Ne particles and three different interaction potentials for pairs of colliding Li–Ar particles, we have studied anomalous LID of Li atoms in an inert buffer Ne gas and in a binary buffer mixture of inert Ne + Ar gases. Theoretical calculations of LID of Li atoms in the buffer Ne gas for the interaction potentials from [32, 33] predict anomalous LID and, as a result, strong sensitivity of the LID line shape of Li atoms to the difference in these interaction potentials. For the three interaction potentials from [30, 31, 34], the LID line shape is insensitive to their difference, since they predict weakly anomalous (close to normal) LID of Li atoms. However, in this case, by adding a small fraction of the buffer Ar gas, one can switch to the region of anomalous LID and thereby radically increase the sensitivity of the LID line shape of Li atoms to the difference of these potentials.

Acknowledgements. The study was supported by the subsidies for the financial support of the fulfilment of the state task (Project No. AAAA-A17-117052210003-4) at the Institute of Automation and Electrometry, Siberian Branch of the Russian Academy of Sciences.

References

1. Gel'mukhanov F.Kh., Shalagin A.M. *Sov. Phys. JETP Lett*., **29**, 711 (1979) [*Pis'ma Zh. Eksp. Teor. Fiz*., **29**, 773 (1979)].
2. Gel'mukhanov F.Kh., Shalagin A.M. *Sov. Phys. JETP*, **51**, 839 (1980) [*Zh. Eksp. Teor. Fiz*., **78**, 1674 (1980)].
3. Rautian S.G., Shalagin A.M. *Kinetic Problems of Nonlinear Spectroscopy* (Amsterdam–New York: Elsevier Science Publ. Comp., 1991).
4. Nienhuis G. *Phys. Rep*., **138**, 151 (1986).
5. Werij H.G.C., Woerdman J.P. *Phys. Rep*., **169**, 145 (1988).
6. Chapovsky P.L. *Izv. Akad. Nauk, Ser. Fiz.*, **53**, 1069 (1989).
7. Eliel E.R. *Adv. At. Mol. Opt. Phys*., **30**, 199 (1992).
8. Nagels B., Chapovsky P.L., Hermans L.J.F., van der Meer G.J., Shalagin A.M. *Phys. Rev. A*, **53**, 4305 (1996).
9. Van Duijn E.J., Nokhai R., Hermans L.J.F. *J. Chem. Phys*., **105**, 6375 (1996).
10. Popov A.K., Shalagin A.M., Shalaev V.M., Yakhnin V.Z. *Sov. Phys. JETP*, **53**, 1134 (1981) [*Zh. Eksp. Teor. Fiz*., **80**, 2175 (1981)].
11. Atutov S.N., Ermolaev I.M., Shalagin A.M. *Sov. Phys. JETP*, **65**, 679 (1987) [*Zh. Eksp. Teor. Fiz*., **92**, 1215 (1987)].
12. Van der Meer G.J., Smeets J., Pod'yachev S.P., Hermans L.J.F. *Phys. Rev. A*, **45**, R1303 (1992).
13. Van der Meer G.J., Broers B., Chapovsky P.L., Hermans L.J.F. *J. Phys. B*, **25**, 5359 (1992).
14. Chapovsky P.L., van der Meer G.J., Smeets J., Hermans L.J.F. *Phys. Rev. A*, **45**, 8011 (1992).
15. Van der Meer G.J., Smeets J., Eliel E.R., Chapovsky P.L., Hermans L.J.F. *Phys. Rev. A*, **47**, 529 (1993).
16. Van Duijn E.J., Bloemink H.I., Eliel E.R., Hermans L.J.F. *Phys. Lett. A*, **184**, 93 (1993).
17. Kuščer I., Hermans L.J.F., Chapovsky P.L., Beenakker J.J.M., van der Meer G.J. *J. Phys. B*, **26**, 2837 (1993).
18. Yahyaei-Moayyed F., Streater A.D. *Phys. Rev. A*, **53**, 4331 (1996).
19. Gel'mukhanov F.Kh., Parkhomenko A.I. *Phys. Lett. A*, **162**, 45 (1992).
20. Gel'mukhanov F.Kh., Parkhomenko A.I. *JETP*, **75**, 225 (1992) [*Zh. Eksp. Teor. Fiz*., **102**, 424 (1992)].
21. Gel'mukhanov F.Kh., Kharlamov G.V., Rautian S.G. *Opt. Commun*., **94**, 521 (1992).
22. Gel'mukhanov F.Kh., Parkhomenko A.I. *J. Phys. B*, **28**, 33 (1995).
23. Gel'mukhanov F.Kh., Parkhomenko A.I., Privalov T.I., Shalagin A.M. *J. Phys. B*, **30**, 1819 (1997).
24. Parkhomenko A.I. *JETP*, **88**, 913 (1999) [*Zh. Eksp. Teor. Fiz*., **115**, 1664 (1999)].
25. Parkhomenko A.I. *JETP*, **89**, 856 (1999) [*Zh. Eksp. Teor. Fiz*., **116**, 1587 (1999)].
26. Parkhomenko A.I., Shalagin A.M. *Quantum Electron*., **43**, 162 (2013) [*Kvantovaya Elektron*., **43**, 162 (2013)].
27. Parkhomenko A.I., Shalagin A.M. *Zh. Eksp. Teor. Fiz*., **145**, 223 (2014).
28. Parkhomenko A.I., Shalagin A.M. *Quantum Electron*., **44**, 928 (2014) [*Kvantovaya Elektron*., **44**, 928 (2014)].
29. Parkhomenko A.I., Shalagin A.M. *Zh. Eksp. Teor. Fiz*., **154**, 300 (2018).
30. Pascale J., Vandeplanque J. *J. Chem. Phys*., **60**, 2278 (1974).
31. Behmenburg W., Kaiser A., et al. *J. Phys. B*, **31**, 689 (1998).
32. Zanuttini D., Jacquet E., Giglio E., Douady J., Gervais B. *J. Chem. Phys*., **131**, 214104 (2009).
33. Blank L.A., Kedziora G.S., Weeks D.E. *Proc. SPIE*, **7581**, 75810I (2010).
34. Bouchoucha S., Alioua K., Bouledroua M. *Chinese Phys. B*, **26**, 073202 (2017).
35. Park S.J., Lee Y.S., Jeung G.-H. *Chem. Phys. Lett*., **277**, 208 (1997).
36. Radzig A.A., Smirnov B.M. *Reference Data on Atoms, Molecules, and Ions* (Berlin: Springer, 1985; Moscow: Energoatomizdat, 1986).
37. Sobel'man I.I. *Introduction to the Theory of Atomic Spectra* (Oxford: Pergamon, 1972; Moscow: Nauka, 1977).
38. Gel'mukhanov F.Kh., Il'ichov L.V., Shalagin A.M. *Physica A*, **137**, 502 (1986).
39. NIST Atomic Spectra Database: https://www.nist.gov/pml/atomic-spectra-database.
40. Allard N., Kielkopf J. *Rev. Mod. Phys*., **54**, 1103 (1982).
41. Atutov S.N., Parkhomenko A.I., Pod'yachev S.P., Shalagin A.M. *J. Phys. B*, **25**, 2943 (1992).
42. Atutov S.N., Bondarev B.V., Kobtzev S.M., Kolinko P.V., Pod'yachev S.P., Shalagin A.M. *Opt. Commun*., **115**, 276 (1995).
43. Gel'mukhanov F.Kh., Shalagin A.M. *Sov. Phys. JETP.*, **50**, 234 (1979) [*Zh. Eksp. Teor. Fiz*., **77**, 461 (1979)].
44. Parkhomenko A.I., Shalagin A.M. *Quantum Electron*., **45**, 131 (2015) [*Kvantovaya Elektron*., **45**, 131 (2015)].